

# $\pi^+\pi^-$ Emission in High-Energy Nuclear Collisions

Ralf Rapp

*NORDITA, Blegdamsvej 17, DK-2100 Copenhagen, Denmark*

Realistic vacuum  $\pi\pi$  interactions are employed to investigate thermal  $\pi^+\pi^-$  emission spectra from the late stages of heavy-ion reactions at ultrarelativistic energies. Hadronic in-medium effects, including many-body  $\rho$ -meson spectral functions used earlier to describe the dilepton excess observed at CERN-SPS energies, are implemented to assess resulting modifications in relation to recent measurements of  $\pi^+\pi^-$  invariant-mass spectra by the STAR collaboration in  $p$ - $p$  and  $Au$ - $Au$  collisions at  $\sqrt{s_{NN}}=200$  GeV. Statistical model estimates for the  $\rho^0/\pi^-$  and  $K^*/K$  ratios close to the expected thermal freezeout are also given.

## I. INTRODUCTION

The unambiguous identification of hadron modifications in hot and/or dense matter constitutes one of the major objectives in modern nuclear physics [1,2]. Hadronic states whose vacuum properties are related to the spontaneous breaking of chiral symmetry, are of particular interest as changes in their spectral distribution reflect precursor phenomena towards the chiral phase transition. A versatile environment for these investigations is provided by high-energy heavy-ion collisions, as different center-of-mass ( $CM$ ) energies have been shown [3] to probe large regions in temperature and density of the QCD phase diagram.

On the one hand, dilepton observables [4–6] have been proved to be powerful tools to extract medium modifications of vector-mesons [2] during the evolution history of the hot and dense fireballs formed in heavy-ion reactions. However, the relative signal weakness (parametrically suppressed by  $\alpha^2$  compared to hadronic sources) entails appreciable experimental uncertainties, which, as of now, do not allow for a unique theoretical interpretation of the results. On the other hand, hadronic final state measurements of strongly decaying resonances have thus far not revealed significant medium effects [7,8]. This is believed to be mostly due to the diluteness of the matter from which the decay products are able to reach the detectors undistorted (unlike in the dilepton case). In this context, recent (preliminary) data [9] on  $\pi^+\pi^-$  invariant-mass distributions from  $\sqrt{s_{NN}}=200$  GeV nuclear collisions by the STAR collaboration are of particular interest. Assuming Breit-Wigner parametrizations of the underlying resonance structures ( $\rho$ ,  $\omega$ ,  $f_0$ , etc.), a downward shift of  $\sim 30$  MeV for the peak position in the  $\pi^+\pi^-$  distribution from  $\rho$ -meson decays has been reported [9] when going from  $p$ - $p$  to 40-80% central  $Au$ - $Au$  collisions. In addition, a shift of -40 MeV relative to a nominal  $\rho$ -meson mass of 770 MeV has been extracted from the  $p$ - $p$  data.

Two recent articles have specifically addressed these observations (see also Ref. [10] for an earlier study). In Ref. [11], a number of hadronic  $s$ - and  $t$ -channel exchanges between  $\rho$ -mesons and the surrounding matter close to freezeout have been estimated to produce

a  $\sim 50$  MeV downward mass shift, mostly originating from scalar  $t$ -channel exchanges with anti-/baryons (in line with "Brown-Rho" scaling [12]). In Ref. [13] a more generic analysis of the interplay between phase-space, mass-shift and width effects has been carried out, with the latter two implemented via schematic selfenergies in the underlying  $\rho$ -meson spectral function.

In the present article we go beyond these analyses in several respects. We will assess  $\pi^+\pi^-$  spectra based on microscopic  $\pi\pi$  interactions that accurately describe pertinent free scattering phase shifts in  $S$ -,  $P$ - and  $D$ -waves, including hadronic medium modifications through finite-temperature effects on intermediate two-pion states. For the  $\rho$  meson we will also use more advanced in-medium many-body spectral functions which have been constructed and applied in recent years mostly in the context of dilepton production (with fair success, *e.g.*, in reproducing the low-mass excess observed by CERES/NA45), cf. Ref. [2] for a recent review. This is critical for illuminating the important issue to what extent the relative apparent mass shift of about 30 MeV between  $p$ - $p$  and  $Au$ - $Au$  experiments is consistent with such an approach, and what responsible mechanisms are. Another question that will be addressed concerns total  $\rho$ -meson yields, *i.e.*, the  $\rho^0/\pi^-$  ratio and its evolution from chemical to thermal freezeout.

The article is organized as follows. In Sec. II we apply microscopic in-medium  $\rho$  spectral functions to compute thermal  $\pi^+\pi^-$  emission rates at RHIC, including a simple evolution model to assess uncertainties due to freezeout conditions. In Sec. III we establish a relation between thermal emission rates and  $\pi\pi$  scattering amplitudes, and employ a realistic  $\pi\pi$  interaction with (thermal) in-medium effects to evaluate  $S$ -wave (" $\sigma$ ") and  $D$ -wave ( $f_2(1270)$ ) contributions to the emission spectra. In Sec. IV we investigate both spectral shape and magnitude of resonance feeddown to the  $\rho$ -meson yield, as well as its evolution from chemical to thermal freezeout in central heavy-ion collisions. We also comment on the related behavior of the recently measured  $K^*/K$  ratio in the hadronic evolution. In Sec. V we summarize and conclude.

A. The  $\rho$ -Meson in Hot Hadronic Matter

Let us briefly recall the main elements in the calculation of the medium-modified  $\rho$ -meson spectral function along the lines of our previous work [14–16]. At finite temperatures and baryon densities, the  $\rho$ -propagator can be cast into the form

$$D_\rho = \frac{1}{M^2 - (m_\rho^{(0)})^2 - \Sigma_{\rho\pi\pi} - \Sigma_{\rho M} - \Sigma_{\rho B}}. \quad (1)$$

The in-medium selfenergy insertions consist of three parts: (i)  $\Sigma_{\rho\pi\pi}$  encodes the free decay width into 2-pion states which in matter is modified by standard "pion-bar" excitations,  $\Delta N^{-1}$  and  $NN^{-1}$  [17–19,14], extended to finite total 3-momentum [15] as well as finite temperatures (most importantly pion Bosefactors), see also Refs. [20,21]. Effects of pion excitations into higher resonances, as well as interactions with hyperons,  $N^*$ - and  $\Delta^*$ -states, are approximated by using an "effective" nucleon density  $\varrho_N^{eff} = (\varrho_N + \frac{1}{2}\varrho_{B^*})$  [16]; (ii)  $\Sigma_{\rho M}$  describes resonant  $\rho$ -interactions with surrounding  $\pi$ ,  $K$  and  $\rho$  mesons (for resonances with established decays into  $\rho$ 's up to masses  $\sim 1.6$  GeV) [22,23]; (iii)  $\Sigma_{\rho B}$  accounts for the resonant  $\rho$ -interactions with surrounding nucleons, hyperons and baryon resonances [24,14,25,16]. All underlying hadronic vertices (characterized by a coupling constant and hadronic formfactor cutoff) have been constrained by both hadronic and radiative decay branchings. In addition, baryonic contributions have been subjected to a comprehensive fit to photoabsorption data on nucleons and nuclei [26]. This, in particular, leaves no room for additional  $t$ -channel exchanges.

At collider energies (RHIC and LHC) the *net* baryon densities at midrapidity are rather small. However, as pointed out in Ref. [27],  $CP$ -invariance of strong interactions implies that the  $\rho$  meson equally interacts with baryons and anti-baryons. Thus, the relevant quantity for medium effects is the *sum* of baryon and antibaryon densities, *i.e.*,  $\varrho_{B+\bar{B}} = \varrho_B + \varrho_{\bar{B}} \simeq \varrho_{B^*}(1 + \bar{p}/p)$ , where  $\bar{p}/p$  denotes the experimentally measured ratio of antiprotons to protons.

The main medium modification of the resulting  $\rho$  spectral function,  $A_\rho \equiv -2\text{Im}D_\rho$ , consists of a substantial broadening of its resonance shape [16,27], even at moderate temperatures and, more importantly, baryon densities. The pole position, on the other hand, is affected rather little. This is due to the quite generic feature that many-body contributions to the real part of the selfenergy are of varying sign and thus tend to cancel, whereas the imaginary parts are of definite sign and thus strictly add up.

Following Ref. [28], the thermal rate of two-pion emission from neutral  $\rho$  decays per unit four-volume and four-momentum can be written as

$$\frac{dN_{\rho^0 \rightarrow \pi^+\pi^-}}{d^4q d^4x} = \frac{3}{4\pi^4} f^\rho(q_0; \mu_\rho, T) \text{Im}D_\rho(M, q; \mu_B, T) \times \text{Im}\Sigma_{\rho\pi\pi}(M), \quad (2)$$

where  $f^\rho$  denotes the usual Bosefactor (with chemical potential  $\mu_\rho$ ), and  $\text{Im}D_\rho$  depends on temperature, baryon-chemical potential  $\mu_B$  and possibly other (meson-) chemical potentials. If the emitted pions reach the detector undistorted, the imaginary part of the two-pion selfenergy is given by the free decay width,  $-\text{Im}\Sigma_{\rho\pi\pi}^{vac}(M) = m_\rho \Gamma_\rho^{vac}(M)$ , which depends on the invariant  $\rho$ -mass  $M$  only. Using the standard  $\rho\pi\pi$  interaction vertex,

$$\mathcal{L}_{\rho\pi\pi} = g_\rho \bar{\rho}^\mu \cdot (\vec{\pi} \times \partial_\mu \vec{\pi}), \quad (3)$$

its explicit form is (cf., *e.g.*, Refs. [18,14])

$$\text{Im}\Sigma_{\rho\pi\pi} = -\frac{g_\rho^2}{6\pi} \frac{k^3}{M} F_{\rho\pi\pi}(k^2)^2, \quad (4)$$

with  $F_{\rho\pi\pi}$  a (weakly momentum-dependent) hadronic formfactor (which suppresses the selfenergy at large masses  $M$ ), and  $k = (M^2/4 - m_\pi^2)^{1/2}$  the pion decay 3-momentum. An invariant-mass distribution is obtained upon integrating Eq. (2) over the thermal  $\rho$  3-momentum distribution\*,

$$\frac{dN_{\rho \rightarrow \pi\pi}}{d^4x dM} = \frac{6}{\pi} \text{Im}\Sigma_{\rho\pi\pi}(M) M \int \frac{d^3q}{q_0(2\pi)^3} f^\rho(q_0; \mu_\rho, T) \times \text{Im}D_\rho(M, q; \mu_B, T). \quad (5)$$

If one neglects the (typically weak [16,15]) 3-momentum dependence of the in-medium  $\rho$  spectral function, and invokes the nonrelativistic limit for the  $\rho$ -meson (scalar) density [13], one arrives at ( $R \equiv dN/d^4x$ )

$$\frac{dR_{\rho \rightarrow \pi\pi}}{dM} = -\frac{6}{\pi} \frac{g_\rho^2}{6\pi} \frac{k^3}{M} F_{\rho\pi\pi}(k)^2 \times \text{Im}D_\rho(M; \mu_B, T) \left(\frac{MT}{2\pi}\right)^{\frac{3}{2}} e^{-(M-\mu_\rho)/T}. \quad (6)$$

The above expression differs from the corresponding one in Ref. [13] by (i) an additional  $1/M$ -factor (as well as formfactor) in the vacuum width, and (ii) the microscopic

---

\*if momentum acceptance cuts on the detected pions are imposed, the 3-momentum integral in Eq. (5) is subject to nontrivial corrections which will then also depend, *e.g.*, on the collective flow velocity  $\rho$ -meson at the moment of decay.

spectral function, which, most notably, leads to an additional  $M$ -dependence in  $\text{Im}\Sigma_\rho^{tot}$  (appearing in the numerator of the spectral function), which is reminiscent (but not equal) to the free selfenergy.

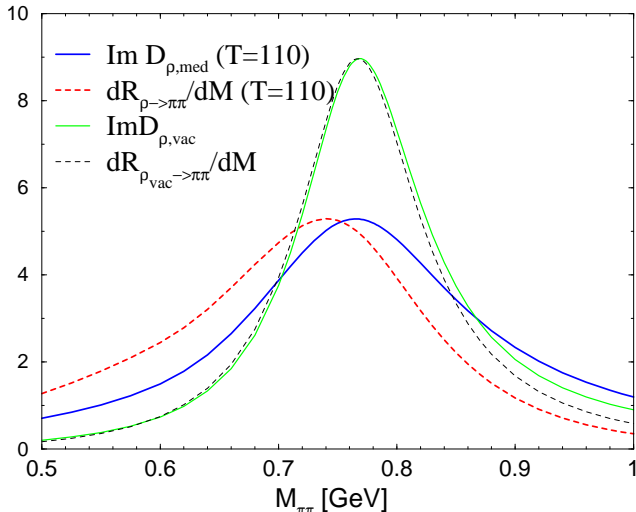


FIG. 1. Comparison of  $\rho$ -meson spectral functions (solid lines, in units of  $\text{GeV}^{-2}$ ) with invariant-mass distributions for  $\rho^0 \rightarrow \pi^+\pi^-$  decay rates (dashed lines, arbitrary units) in an environment characteristic for  $p$ - $p$  (narrow resonance curves) and  $Au$ - $Au$  (broader resonance curves) collisions.

It is instructive to illustrate the impact of the various factors in the  $\pi\pi$  production rate, Eq.(6), relative to the  $\rho$  spectral function, for a static environment, *i.e.*, at fixed temperature and chemical potentials. To represent the  $p$ - $p$  case, we use the vacuum  $\rho$  spectral function and a temperature of  $T = 170$  MeV characteristic for the pertinent hadron production systematics. Comparing the  $\pi\pi$  invariant-mass distribution with the bare spectral function in Fig. 1, one observes a slight shift of about -5 MeV, caused by a competition of the thermal occupation factor (inducing a downward shift) and the various phase space factors (which mostly increase with  $M$  favoring an upward shift). For the  $Au$ - $Au$  case, the appropriate conditions correspond to the thermal freeze-out stages as extracted, *e.g.*, from blast wave fits to hadron  $p_t$ -spectra. We here adopt the parameters determined by hydrodynamic calculations [29] based on suitably constructed chemical-off-equilibrium hadronic trajectories [30], yielding  $T \simeq 110$  MeV,  $\mu_\pi = 0.5\mu_\rho \simeq 90$  MeV,  $\mu_N \simeq 365$  MeV, etc., translating into a total baryon+antibaryon density  $\varrho_{B+\bar{B}} = 0.24\varrho_0$ . We first note that, under these conditions, the  $\rho$  spectral function is still appreciably broadened, which, after multiplying with phase space and thermal factors, results in a  $\sim 25$  MeV relative shift of the maximum in the  $\pi\pi$  invariant-mass distribution, cf. Fig. 1. The rather low temperature also induces a significant shape distortion which leads to a more pronounced "apparent" resonance

shift, in the following sense: when evaluating the shift of the resonance curves at the full-width half-maximum (FWHM), it amounts to about -45 MeV on *both* sides of the resonance.

For a more realistic description of the emitted (undistorted) pion pairs from the late stages of a heavy-ion collision one should allow for a finite emission duration over a profile in temperature and density around the expected (average) freezeout conditions. A simplified way to do this is using a schematic thermal fireball model based on cylindrical volume expansion with parameters consistent with experiment. The space-time integrated emission rate then becomes

$$\begin{aligned} \frac{dN_{\rho \rightarrow \pi\pi}}{dM} &= \frac{3}{\pi^3} \text{Im}\Sigma_{\rho\pi\pi}(M) M \int_{t_0}^{\infty} dt V_{FB}(t) P(t, t_{max}) \\ &\times \int \frac{q^2 dq}{q_0} f^\rho(q_0; T(t), \mu_\rho(t)) \\ &\times \text{Im}D_\rho(M, q; \mu_B(t), T(t)) \text{Acc}(M, q), \quad (7) \end{aligned}$$

where  $V_{FB}(t)$  denotes the time-dependent (isotropic) volume,  $\text{Acc}(M, q)$  accounts for experimental acceptance, and the function  $P(t, t_{max})$  represents the probability distribution of  $\pi^+\pi^-$  emission around the "average" freezeout. For illustration purposes we here assume a Gaussian profile,

$$P(t, t_{max}) = P_0 \exp\left[-(t - t_{max})^2 / 2\sigma_t^2\right] \quad (8)$$

with  $t_{max}$  the time of maximal emission, a width characterized by  $\sigma_t$  and a (dimensionless) constant  $P_0 \leq 1$ . A more detailed treatment with explicit inclusion of pion absorption effects will be given elsewhere [31]. In combination with the increasing fireball volume,  $V_{FB}(t)$ , the resulting emission time profile resembles the example given in Ref. [11] based on hydrodynamical estimates. The resulting  $\pi\pi$  invariant-mass spectra shown in Fig. 2 are computed with  $\sigma_t = 1$  fm/c and  $P_0 = 0.5$  (translating into an effective emission duration  $\Delta t \simeq 1.25$  fm/c), as well as for two average freezeout temperatures (with appropriate pion-chemical potentials [30]) characteristic for central  $Au$ - $Au$  at full RHIC energy. When employing vacuum  $\rho$  spectral functions, the peak positions are located at about  $M_{\pi\pi} \simeq 760$  MeV (*i.e.*, 10 MeV below the nominal mass), whereas the in-medium broadening effects [16,27] lower the maxima to about  $M_{\pi\pi} \simeq 740$ -745 MeV. Again, the "apparent" mass shift at the center of the FWHM is larger due to the distorted line shape. One can quantify this feature by defining a "centroid" of the mass distribution as

$$(m_{\pi\pi}^{cent})^2 = \int dM M^2 \frac{dN}{dM} / \int dM \frac{dN}{dM}. \quad (9)$$

For the  $\bar{T}=110(125)$  MeV scenario we find  $m_{\pi\pi}^{cent} = 722(739)$  MeV and  $758(769)$  MeV with the in-medium and free  $\rho$  spectral function, respectively. Furthermore,

note that in both cases, the spectral shapes are relatively robust with respect to (w.r.t.) variations in the freezeout temperature, whereas the yield is reduced by  $\sim 20(15)\%$  for the free (in-medium) spectral function. We will return to the latter issue in Sec. IV B.

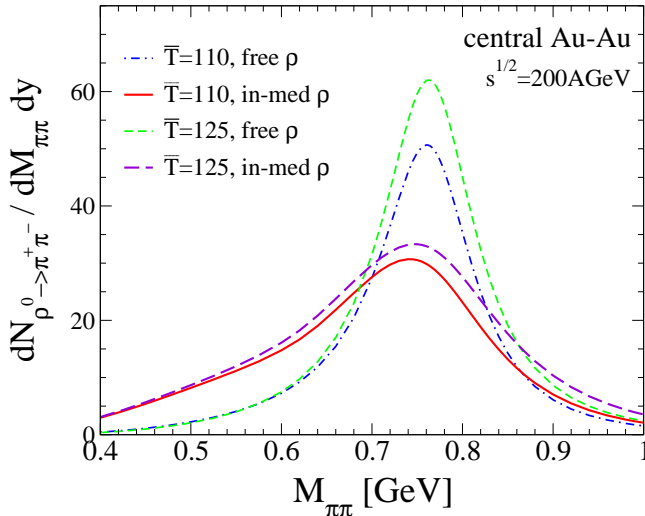


FIG. 2. Time-integrated  $\pi^+\pi^-$  emission spectra from thermal  $\rho^0$ -decays in the late stages of central *Au-Au* collisions at RHIC based on Eqs. (7) and (8). The dashed-dotted (short-dashed) and full (long-dashed) lines are for  $\bar{T} = T(t_{max}) = 110(125)$  MeV using free and in-medium  $\rho$  spectral functions, respectively.

### III. *S*- AND *D*-WAVE $\pi\pi$ CORRELATIONS AND EMISSION

#### A. Microscopic $\pi\pi$ Interactions and Strength Distributions

In addition to direct  $\rho$ -meson decays, a number of other sources of (strongly) correlated  $\pi^-\pi^+$  emission contribute to their invariant-mass distribution. These sources are either due to feeddown from resonances (*e.g.*,  $a_1 \rightarrow \rho\pi$ ) or "direct"  $\pi\pi$  correlations. The former will be addressed in Sect. IV; the latter, which we will focus on now, are determined by the  $\pi\pi$  interaction strength in a given spin-isospin channel; for an isospin-1 *P*-wave ( $JI=11$ ) the strength distribution is essentially saturated by the  $\rho$ -meson (*i.e.*,  $\rho$  decays), but non-resonant contributions are in principle also present. In the *S*-wave,  $\pi\pi$  interactions are sizable for both isoscalar ( $JI=00$ ) and isotensor ( $JI=02$ ) states. The former represent the well-known " $\sigma$ "-channel, with ongoing controversy on the nature of the observed resonance structures. For the emission strength the relevant quantity is the imaginary part of the scattering amplitude, as determined via  $\pi\pi$  scat-

tering phase shifts  $^\dagger$ . In the *D*-wave, the only significant feature is the  $f_2(1270)$  resonance, with little interaction strength below  $M_{\pi\pi} = 1$  GeV.

A microscopic model that accurately reproduces free  $\pi\pi$  scattering in *S*-, *P*- and *D*-waves up to invariant masses of about 1.5 GeV, is the Jülich  $\pi\pi$  interaction [33]. It is based on an effective Lagrangian generating *s*-, *t*- and *u*-channel meson exchanges which are iterated to all orders by solving an underlying Lippmann-Schwinger equation,

$$\mathcal{M}^{JI} = V^{JI} + V^{JI} G_{\pi\pi} \mathcal{M}^{JI}, \quad (10)$$

for the scattering amplitude  $\mathcal{M}^{JI}$ ;  $V^{JI}$  and  $G_{\pi\pi}$  are the two-body potentials (Born amplitudes) and 2-pion propagator, respectively. In the following we employ a chirally improved version [34] thereof, which has been extended by  $\pi\pi$  contact interactions to satisfy constraints from chiral symmetry (these are necessary for a reliable treatment of in-medium effects). In Fig. 3, the solid lines represent the imaginary part of the  $\pi\pi$  scattering amplitude in the " $\sigma$ ",  $\rho$  and  $f_2$  channels as obtained from the Jülich model in vacuum, and including medium effects on the two-pion propagator within a hot pion gas [35] corresponding to RHIC freezeout conditions (direct resonances, such as  $\rho\pi \rightarrow a_1$ , as well as baryonic effects are not accounted for in this Section; a more complete treatment in " $\sigma$ " and  $f_2$  channels will be reported elsewhere).

To obtain the pertinent  $\pi^+\pi^-$  emission rates, two further steps are necessary. First, recalling Eq. (2), the combination of spectral function and decay width has to be related to  $\text{Im}\mathcal{M}$ . Using  $\Sigma_{\rho\pi\pi} = v_\rho G_{\pi\pi} v_\rho$  and  $\mathcal{M}^{11} = v_\rho D_\rho v_\rho$  ( $v_\rho$ :  $\rho\pi\pi$  vertex function), one obtains

$$\text{Im}D_\rho \text{Im}\Sigma_\rho = \text{Im}\mathcal{M}^{11} \text{Im}G_{\pi\pi} \quad (11)$$

with  $\text{Im}G_{\pi\pi} = k/(16\pi M)$ . Second, the isospin basis has to be transformed into particle basis for the two outgoing pions. For  $|II_z\rangle = |10\rangle$  states (*i.e.*, neutral  $\rho$ -mesons), the overlap with  $\pi^+\pi^-$  pairs is 100%. For *S*- and *D*-waves, however, isospin  $I=0$  and  $I=2$  states contribute,

$$\mathcal{M}_{\pi^+\pi^-}^J = \frac{2}{3} \mathcal{M}^{J,I=0} + \frac{1}{3} \mathcal{M}^{J,I=2}, \quad (12)$$

with only 2/3 of the " $\sigma$ "- and  $f_2(1270)$ -mesons decaying into  $\pi^+\pi^-$  (the other 1/3 into  $\pi^0\pi^0$ ).

The 3-momentum integrated emission-strength distributions,  $dR^{JI}/dM$ , in the individual spin-isospin channels are shown by the dashed lines in Fig. 3 (in arbitrary normalization). Both  $\rho$ - and  $f_2$ -resonance peaks

$^\dagger$ This is strictly correct only as long as no medium effects are included, since the latter may be quite sensitive to the underlying microscopic interactions (*cf.*, *e.g.*, Refs. [32] for a detailed analysis in cold nuclear matter).

are slightly shifted downward mostly due to the thermal occupation factors, between 10-20(30-40) MeV at  $T=170(110)$  MeV. The broad structure in the  $\sigma$ -channel is more strongly distorted by the thermal weights, with an appreciable shift of strength towards lower masses, especially for the smaller temperature. However, these effects are less pronounced than the ones obtained in Refs. [11,13]. This is a consequence of the schematic  $\sigma$  mass distributions used in those works which imply an overestimation of the (free)  $\pi\pi$  scattering phase shifts, and thus of the low invariant-mass strength, in the scalar-isoscalar channel.

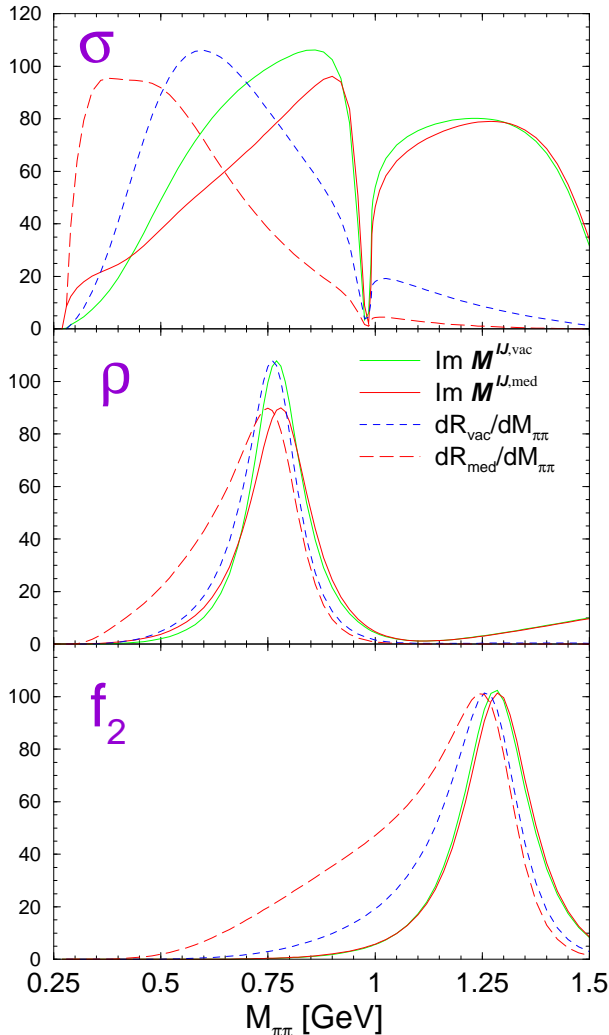


FIG. 3. Imaginary part of  $\pi\pi$  scattering amplitudes within the Jülich model (solid lines; light: in vacuum, dark: including medium effects at  $T=110$  MeV and  $\mu_\pi=90$  MeV) and corresponding  $\pi^+\pi^-$  production rates (arbitrarily normalized; short-dashed line:  $T=170$  MeV with vacuum amplitudes, long-dashed line:  $T=110$  MeV,  $\mu_\pi=90$  MeV with in-medium amplitudes).

## B. Thermal $\pi^+\pi^-$ Emission Spectra

Implementing the relation (11) into Eq. (5), the spin-isospin weighted sum for  $\pi^+\pi^-$  thermal emission rates can be expressed through the  $\pi\pi$  scattering amplitudes in  $S$ -,  $P$ - and  $D$ -waves as

$$\frac{dR_{\pi^+\pi^-}}{dM} = \frac{k}{(2\pi)^4} \int \frac{q^2 dq}{q_0} f^B(q_0; 2\mu_\pi, T) \times \sum_J (2J+1) \text{Im} \mathcal{M}_{\pi^+\pi^-}^J(M; \mu_\pi, T). \quad (13)$$

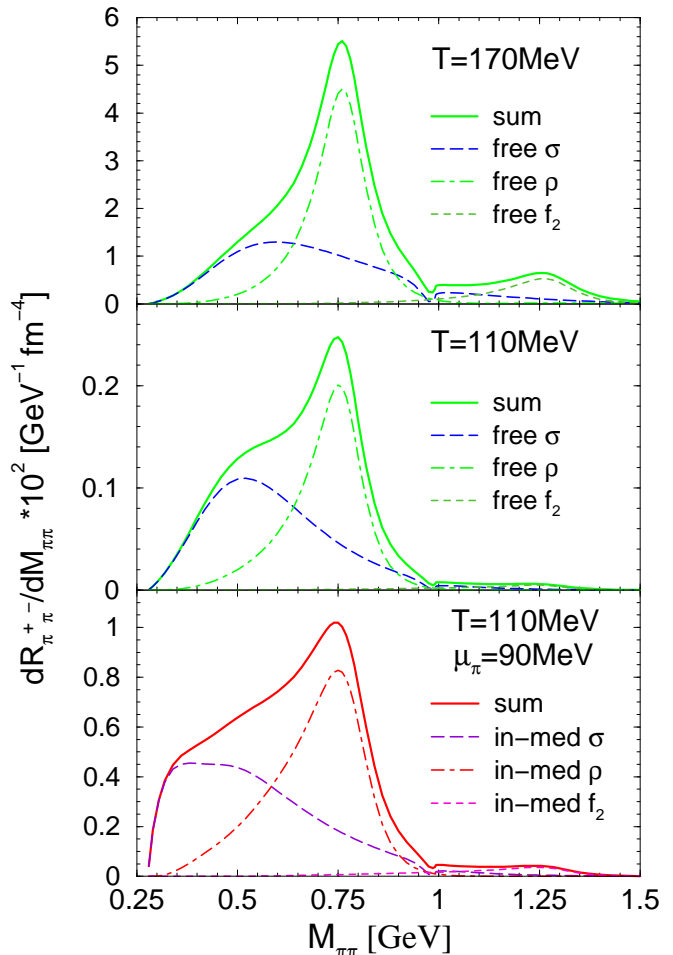


FIG. 4. Thermal  $\pi^+\pi^-$  emission rates employing the Jülich model scattering amplitudes of Fig. 3. Upper and middle panel: using free  $\pi\pi$  amplitudes at  $T=170$  MeV and  $T=110$  MeV, respectively, and  $\mu_\pi=0$ ; lower panel: using in-medium amplitudes with finite- $T$  pion modifications [35] at  $T=110$  MeV and  $\mu_\pi=90$  MeV.

The combined results of the Jülich  $\pi\pi$  interaction from Fig. 3 are displayed in Fig. 4 for temperatures and pion-chemical potentials believed to resemble freezeout conditions in  $p$ - $p$  and central  $Au$ - $Au$  collisions. At  $T=170$  MeV

(upper panel), where free  $\pi\pi$  amplitudes have been employed, the spectrum is dominated by the  $\rho$  resonance with a slight low-mass shoulder from scalar correlations, and a clearly discernible  $f_2$  resonance. The maximum of the  $\rho$  peak is located at  $M_{\pi\pi} = 760$  MeV. Reducing the emission temperature to  $T=110$  MeV, the stronger distortion of the " $\sigma$ " increases the low-mass shoulder, whereas the relative height of the  $f_2$  peak is suppressed. Also note that the  $\rho$  resonance is situated on the decreasing slope of the " $\sigma$ " distribution, which entails an additional apparent 5-10 MeV downward shift of its position. The lower panel in Fig. 4 finally incorporates finite- $T$  in-medium effects on the pions in the scattering amplitudes [35], as well as finite meson-chemical potentials (as inferred from chemistry-conserving thermodynamic trajectories [30]). One observes a reinforced threshold enhancement, as well as a net shift of the  $\rho$ -peak by about -25 MeV, (recall that baryonic medium effects, as well as direct  $\rho$ -hadron resonances, are not included here).

Another noteworthy feature is the minimum structure in the  $f_0(980)$  resonance region, which is a direct consequence of the  $180^\circ$ -crossing of the scalar-isoscalar  $\pi$ - $\pi$  phase shifts, *i.e.*, the coherence in formation and decay process of the  $f_0$  (this is different for the " $\sigma$ ",  $\rho$  and  $f_2$  resonances, which induce the usual  $90^\circ$ -crossing). If, on the contrary, a  $\pi\pi$  resonance structure is observed in the  $f_0(980)$  region (as, *e.g.*, in  $pp$  collisions [9]), it seems to require a different production mechanism, such as string breaking. More subtle effects associated with the controversial nature of the  $f_0(980)$  might also play a role [36], *e.g.*, formation through the  $K\bar{K}$  channel.

### C. Final-State Bose-Einstein Correlations

Apparent mass shifts of  $\rho$  resonances detected via the  $\pi\pi$  channel are a well-known phenomenon in elementary  $p$ - $p$  collisions and hadronic jets in  $e^+e^-$  annihilation at high energy. Among the possible explanations [37] are interferences between direct and secondary (through  $\pi$ - $\pi$  rescattering)  $\rho$  production, as well as phase space distortions due to Bose-Einstein correlations between the decay-pions and the surrounding ones. Whereas the role of the former might be reduced in heavy-ion collisions, the opposite can be expected for the latter.

A naive way of introducing statistical final-state correlations (which were not addressed in Refs. [10,11,13]) into the thermal emission rate consists of modifying the free final-state  $\pi\pi$  decay by an extra Bosefactor, *i.e.*, implementing a factor  $[1 + 2f^\pi(\omega_k; T)]$  into  $\text{Im}\Sigma_{\rho\pi\pi}$  in Eq. (5). However, this procedure neglects the dependence on the total three-momentum  $q$  of the pion-pair (w.r.t. the thermal frame). A better approximation is obtained by performing an angular average according to [38]

$$\langle 1 + f^\pi(\vec{k}; T) + f^\pi(-\vec{k}; T) \rangle =$$

$$\begin{aligned} &= \frac{1}{2} \int_{-1}^{+1} d\cos\theta [1 + f^\pi(\vec{k}'_+; T) + f^\pi(\vec{k}'_-; T)] \\ &= \frac{T}{\beta\gamma k} \ln \left\{ \frac{\sinh\left(\frac{1}{2T}[\gamma(\omega_k + \beta k) - \mu_\pi]\right)}{\sinh\left(\frac{1}{2T}[\gamma(\omega_k - \beta k) - \mu_\pi]\right)} \right\} \end{aligned} \quad (14)$$

which depends on the pair 3-momentum and invariant-mass through the Lorentz factors  $\beta=q/q_0$  and  $\gamma=q_0/M_{\pi\pi}$  ( $\vec{k}'_\pm$  are the pion momenta in the thermal rest frame). Consequently,  $\text{Im}\Sigma_{\rho\pi\pi}$  in Eq. (5) has to be evaluated inside the momentum integral. An upper estimate of the final-state Bose correlations may be obtained by inserting the same temperature and chemical potentials as in the spectral function in Eq. (5). This leads to an appreciable impact on the  $\pi^+\pi^-$  emission spectra, cf. Fig. 5: in the  $\rho$ -resonance region, the rate increases by 20 % ("stimulated" emission), accompanied by a small downward move (5-10 MeV) of the peak position. Towards the two-pion threshold, a more pronounced " $\sigma$ " shoulder emerges. The finite- $q$  corrections moderate the Bose enhancement close to the two-pion threshold, most notably for low temperature and large pion-chemical potential.

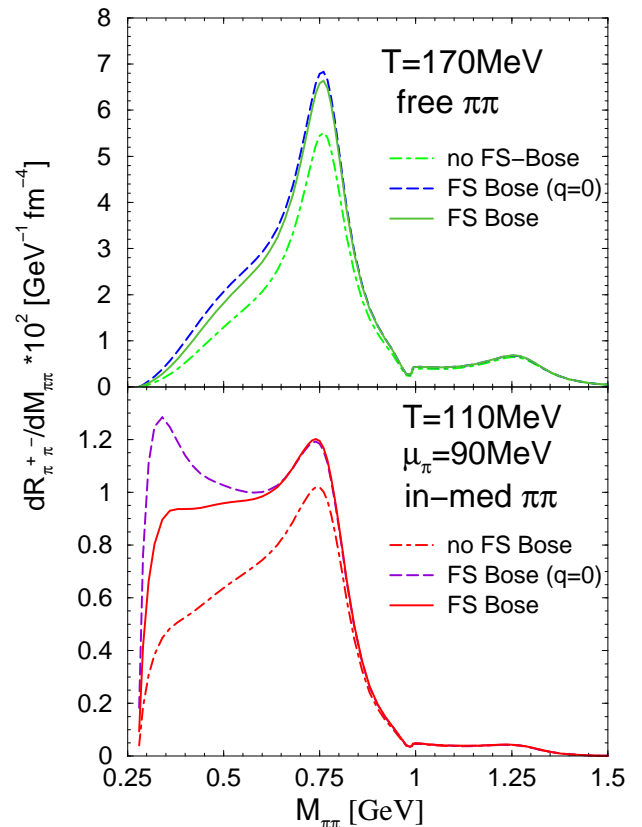


FIG. 5. Thermal  $\pi^+\pi^-$  emission rates employing the Jülich model scattering amplitudes with additional account for final-state Bose-Einstein enhancement. Dashed-dotted lines represent the results of Sec. IIIB (solid lines in Fig. 4), whereas solid and dashed lines include the final-state Bose-factors with and without finite- $q$  corrections, respectively.

#### IV. RESONANCE FEEDDOWN AND RATIOS

We now return to the question of feeddown contributions to  $\pi^+\pi^-$  distributions, concerning both their magnitude and spectral shape. For simplicity, we will focus on the  $\rho$  meson, which is well-established in a large number of mesonic and baryonic resonance-decay branchings (less so for the scalar " $\sigma$ "- and tensor  $f_2$ -mesons).

##### A. Spectral $\pi\pi$ Shape from $a_1$ Decays

As a typical example for resonance feeddown, we here concentrate the  $a_1(1260) \rightarrow \rho\pi$  decay (which gives the largest individual contribution). Starting point is the 3-momentum integrated emission rate, Eq. (6), which for the present case takes the form

$$\frac{dR_{a_1 \rightarrow \rho\pi}}{dM_a} = \frac{6}{\pi} \text{Im}\Sigma_{a_1\rho\pi}(M_a) \text{Im}D_{a_1}(M_a; \mu_B, T) \times \left(\frac{M_a T}{2\pi}\right)^{3/2} e^{-(M_a - \mu_{a_1})/T}. \quad (15)$$

The  $a_1\rho\pi$  selfenergy is related to the pertinent partial decay width via  $-\text{Im}\Sigma_{a_1\rho\pi} = M_a \Gamma_{a_1 \rightarrow \rho\pi}$ . Including the  $\rho$ -mass distribution through its spectral function  $A_\rho(M)$ , one has

$$\Gamma_{a_1 \rightarrow \rho\pi}(M_a) = \frac{1}{12\pi M_a^2} \int_{2m_\pi}^{M_{max}} \frac{M dM}{\pi} A_\rho(M) q_{cm} v_{\rho\pi a_1}^2, \quad (16)$$

where  $q_{cm}$  denotes the three-momentum of the decay products  $\rho$  (mass  $M$ ) and  $\pi$  (mass  $m_\pi$ ) in the  $a_1$  rest frame,  $v_{\rho\pi a_1}$  the vertex function, and  $M_{max} = M_a - m_\pi$ . Using the differential form of Eq. (16), and integrating Eq. (15) over the  $a_1$ -mass distribution, yields the  $\rho$ -like  $\pi^+\pi^-$  production rate from  $a_1$  decays as

$$\frac{dR_{a_1 \rightarrow \pi(\pi^+\pi^-)}}{dM} = -\frac{6}{\pi} \int dM_a M_a \int \frac{d^3k}{(2\pi)^3} \frac{M_a}{k_0} \frac{d\Gamma_{a_1 \rightarrow \rho\pi}}{dM} \times f^{a_1}(k_0; \mu_{a_1}, T) \text{Im}D_{a_1}(M_a, k; \mu_B, T), \quad (17)$$

where we reintroduced the explicit integration over the  $a_1$  Bose function,  $f^{a_1}$ , with  $k_0 = (M_a^2 + k^2)^{1/2}$ . An important ingredient in evaluating Eq. (17) is the  $a_1$  spectral function; we use a microscopic description with a  $\rho\pi$  selfenergy which gives an accurate description of recent axialvector  $\tau$ -decay data.

It turns out that the resulting  $\pi^+\pi^-$  mass distributions are not much affected (downward peak-shifts of 5-10 MeV even at low temperatures), which is primarily due to the fact that the *free*  $\rho$  spectral function enters into the expression for the  $a_1$ -decay width, Eq. (16). Broadening effects in the underlying  $a_1$  spectral function have very

little impact either. Final-state Bose enhancement factors, implemented along the lines of Sec. III C, can lead to net peak-shifts of maximally -15 MeV. Note that the relative contribution from resonance feeddown is expected to decrease with decreasing temperatures.

##### B. $\rho/\pi$ and $K^*/K$ Ratios

For a thermal hadron gas at  $T = 180$  MeV in full chemical equilibrium, an additional  $\sim 60\%$  of the equilibrium  $\rho$ -number will emerge from resonance feeddown (this excludes subthreshold contributions of the type  $\omega \rightarrow \rho\pi$  or  $N(1520) \rightarrow N\rho$  which do not feed into the  $\rho$ -meson peak); the largest component of about 13% each arises from  $a_1(1260) \rightarrow \rho\pi$  and  $a_2(1320) \rightarrow \rho\pi$  decays (at  $\mu_B = 0$ , about 10% arise from anti-/baryon decays). The resulting  $\rho^0/\pi^-$  ratio ranges between 0.106 and 0.125 depending on whether weak decays are included in the  $\pi^-$  yield or not. Such values are in good agreement with previous measurements in  $e^+e^-$  and  $pp$  collisions at  $\sqrt{s} \simeq 10$ -100 GeV. The recent (preliminary) STAR measurement for  $\sqrt{s} = 200$  GeV  $pp$  reports  $\rho^0/\pi^- = 0.173 \pm 0.026$  [9]. This value, however, does not account for the possibility that other  $\pi^+\pi^-$  sources (most notably " $\sigma$ " correlations) may "contaminate" the  $\rho$  resonance region. From the upper panel of Fig. 4 one infers that this could lead to a up to 20% correction of the  $\rho^0$  yield.

An important question is how the  $\rho^0/\pi^-$  ratio develops when going to (central) heavy-ion collisions. The  $\rho$  meson constitutes one of the strongest agents for pion interactions, and thus for maintaining thermal equilibrium. This means that  $\rho \leftrightarrow \pi\pi$  stays in relative chemical equilibrium, and therefore  $\mu_\rho = 2\mu_\pi$ . Finite  $\mu_\pi$ 's build up between chemical and thermal freezeout due to effective pion-number conservation (and likewise for kaons, etas, and even antibaryons), cf. Ref. [30] for a hadronic evolution (*i.e.*, thermodynamic trajectory) under RHIC conditions. To obtain the total number of  $\rho^0$  and  $\pi^-$  in the later stages one again has to include the feeddown corrections of all the resonances, but with their respective (effective) chemical potentials (*e.g.*,  $\mu_{a_1} = \mu_\rho + \mu_\pi = 3\mu_\pi$ , etc.). Starting the evolution from chemical freezeout at  $(\mu_\pi, T) = (0, 180)$  MeV, the  $\rho^0/\pi^-$  ratio is first almost stable, being reduced by only 15% at  $(\mu_\pi, T) = (60, 140)$  MeV. It then starts falling faster being reduced by 30% at  $(\mu_\pi, T) = (85, 120)$  MeV, *i.e.*,  $\rho^0/\pi^- = 0.075$ -0.087, and to 0.05-0.06 at  $(\mu_\pi, T) = (100, 100)$  MeV. These ranges thus characterize (equilibrium-) conditions close to thermal decoupling in central  $Au$ - $Au$  collisions. The (preliminary) STAR measurement in peripheral  $Au$ - $Au$  lies significantly higher, at  $0.183 \pm 0.027$  [9]. Again,  $\pi\pi$   $S$ -wave contributions in the spectra could lower this value. Also, the actually detected number of  $\rho^0 \rightarrow \pi^+\pi^-$  decays might be affected by an interplay between (pion-) absorption and ( $\rho^0$ -) regeneration in the vicinity of ther-

mal freezeout. Here, transport simulations should be an adequate tool, which find a  $\rho^0/\pi^-$  ratio of around 8% [39].

Let us briefly comment on a closely related quantity that has recently been measured at RHIC energies, namely the  $K^*(892)/K$  ratio. For 200 GeV  $p$ - $p$  collisions STAR obtained  $0.386\pm 0.029$  (preliminary), to be compared to a statistical model value of 0.35-0.36 at  $T=180$  MeV. For 0-10% (0-14%) central  $Au$ - $Au$  at 200 (130) AGeV, the ratio was found to decrease to  $0.205\pm 0.033$  ( $0.26\pm 0.07$ ) [40,41]. On the one hand, it has been argued that this implies, based on the vacuum  $K^*$  lifetime of about 4 fm/c, an upper limit on the duration of the hadronic phase, which follows if one assumes no regeneration. If, on the other hand, the reaction  $K^* \leftrightarrow K\pi$  is assumed to maintain (relative) chemical equilibrium, one has  $\mu_{K^*} = \mu_\pi + \mu_K$ . Along the thermodynamic trajectory discussed above one then finds the  $K^*/K$  ratio to slowly decrease, passing through values of 0.235-0.295 at temperatures  $T=100$ -120 MeV (and  $\mu_{mes}>0$ ). Thus, even complete regeneration (which, in the denser stages, could be facilitated by in-medium broadening effects) cannot be ruled out by the current measurements. The same pattern emerges for the  $K^{0^*}/h^-$  ratio. The preliminary STAR value for 0-20% (0-14%) central  $Au$ - $Au$  at 200 (130) AGeV is  $0.033\pm 0.004$  ( $0.042\pm 0.011$ ) [9,41]. For the hadron gas value at chemical freezeout ( $T=180$  MeV) we find  $K^{0^*}/h^-=0.041$ , in good agreement with the statistical model values of Ref. [42]. Around thermal freezeout ( $T=100$ -120 MeV) the equilibrium ratio has decreased to  $K^{0^*}/h^-=0.028$ -0.035.

## V. SUMMARY AND CONCLUSIONS

In the present article we have investigated spectral shapes and yields of  $\pi^+\pi^-$  invariant-mass spectra arising from thermal sources characteristic for the decoupling stages of high-energy heavy-ion collisions. Our analysis is based on realistic  $\pi\pi$  interactions in  $S$ -,  $P$ - and  $D$ -waves, adjusted to free scattering phase shifts.

For the  $P$ -wave, in line with previous studies [11,13], thermal phase-space factors were found to induce up to 10 MeV downward shifts of the  $\rho$ -peak position when assuming the vacuum resonance profile. However, when using microscopic in-medium  $\rho$  spectral functions, for which a broadening of about 80-100 MeV in dilute hadronic matter has been predicted earlier, the combination with thermal  $\pi\pi$  phase space leads to a peak-mass reduction of about 30 MeV. In fact, low-mass tails of the  $\pi\pi$  distribution lower its centroid by up to another 20 MeV. These findings are more pronounced than the corresponding ones of Ref. [13] (based on schematic spectral functions). Although the effects of in-medium modifications qualitatively reflect the relative changes between  $p$ - $p$  and  $Au$ - $Au$  collisions as extracted from preliminary STAR data [9], the experimentally observed absolute peak shifts of about

-40 MeV and -70 MeV, respectively, are not reproduced by our results.

For  $S$ -wave emission, especially in the scalar-isoscalar (" $\sigma$ ") channel, we emphasized the importance of employing realistic  $\pi\pi$  scattering amplitudes (strength distributions), which sensitively respond to distortions by thermal occupation factors close to freezeout. This is mandatory for a reliable assessment of in-medium effects on the " $\sigma$ ", which, as for the  $\rho$ , can be related to partial chiral symmetry restoration. We found that thermal medium modifications and pion Bose-enhancement lead to an extended threshold maximum ( $M_{\pi\pi}=300$ -500 MeV) in the  $S$ -wave  $\pi^+\pi^-$  emission rates. However, its magnitude relative to the  $P$ -wave contribution is moderate, translating into a low-mass shoulder of the  $\rho$  resonance. In addition, the decreasing " $\sigma$ " slope in the  $\rho$ -resonance region induces another -10 MeV apparent shift of the observed  $\rho$  peak. The general trend in the preliminary STAR data which indicates a decrease in the height of the  $\rho$ -peak relative to the low-mass continuum when going from  $p$ - $p$  to  $Au$ - $Au$  collisions, is qualitatively reproduced by our results. To what extent this reflects a  $\rho$  broadening, and what *additional* mass shift is required, should be evaluated by a more quantitative comparison to experimental spectra.

Finally, we have assessed total  $\rho^0$  yields, including feeddown corrections. We found that the hadrochemical freezeout value for the  $\rho^0/\pi^-$  ratio ( $\sim 11\%$  at  $T=180$  MeV) decreases by only about 30-40% towards thermal freezeout ( $T=110$ -120 MeV), due to large pion-chemical potentials.

For future investigations, a more complete treatment of in-medium effects on the " $\sigma$ ", combining finite temperatures and densities, is desirable. The  $f_0(980) \rightarrow \pi^+\pi^-$  contribution clearly deserves further study. For a realistic comparison with experimental data, Dalitz decays (*e.g.*,  $\omega \rightarrow (\pi^+\pi^-)\pi^0$ ) have to be included. Also, pion absorption effects need to be addressed explicitly. In addition, the relation to resonance modifications in high-energy  $pp$  and  $e^+e^-$  collisions ought to be understood better [37]. Only an overall consistent treatment will eventually allow for a reliable extraction of in-medium effects from short-lived resonance spectroscopy in the heavy-ion environment.

## ACKNOWLEDGMENTS

I thank G.E. Brown, P. Fachini and Z. Xu for interesting discussions, and P. Fachini for bringing Ref. [37] to my attention.

---

[1] G.E. Brown and M. Rho, Phys. Rept. **363** (2002) 85.

- [2] R. Rapp and J. Wambach, *Adv. Nucl. Phys.* **25** (2000) 1.
- [3] P. Braun-Munzinger, K. Redlich and J. Stachel, *nucl-th/0304013*.
- [4] CERES Collaboration (G. Agakichiev *et al.*), *Phys. Rev. Lett.* **75** (1995) 1272; *Phys. Lett.* **B422** (1998) 405.
- [5] HELIOS-3 Collaboration (A.L.S. Angelis *et al.*), *Eur. Phys. J.* **C5** (1998) 63.
- [6] CERES/NA45 Collaboration (D. Adamova *et al.*), *nucl-ex/0209024*; *Nucl. Phys.* **A715** (2003) 262.
- [7] E917 Collaboration (B.B. Back *et al.*), *Nucl. Phys.* **A661** (1999) 506.
- [8] NA49 Collaboration (S.V. Afanasev *et al.*), *Phys. Lett.* **B491** (2000) 59.
- [9] STAR Collaboration (P. Fachini *et al.*), *Nucl. Phys.* **A715** (2003) 462; *Proc. of "7. Int. Conference on Strangeness in Quark Matter"* (12.-17.03.03, Atlantic Beach, NC), to be published in *J. Phys.* **G**.
- [10] H.W. Barz, G. Bertsch, B.L. Friman, H. Schulz and S. Boggus, *Phys. Lett.* **B265** (1991) 219.
- [11] E.V. Shuryak and G.E. Brown, *Nucl. Phys.* **A717** (2003) 322.
- [12] G.E. Brown and M. Rho, *nucl-th/0206021*.
- [13] P.F. Kolb and M. Prakash, *Phys. Rev.* **C67** (2003) 044902.
- [14] R. Rapp, G. Chanfray and J. Wambach, *Nucl. Phys.* **A617** (1997) 472.
- [15] M. Urban, M. Buballa, R. Rapp and J. Wambach, *Nucl. Phys.* **A641** (1998) 433; *ibid.* **A673** (2000) 357.
- [16] R. Rapp and J. Wambach, *Eur. Phys. J.* **A6** (1999) 415.
- [17] M. Asakawa, C.M. Ko, P. Levai and X.J. Qiu, *Phys. Rev.* **C46** (1992) 1159.
- [18] G. Chanfray and P. Schuck. *Nucl. Phys.* **A555** (1993) 329.
- [19] M. Herrmann, B. Friman and W. Nörenberg, *Nucl. Phys.* **A560** (1993) 411.
- [20] H. van Hees and J. Knoll, *Nucl. Phys.* **A683** (2000) 369.
- [21] M. Urban, M. Buballa and J. Wambach, *Phys. Rev. Lett.* **88** (2002) 042002.
- [22] R. Rapp and C. Gale, *Phys. Rev.* **C60** (1999) 024903.
- [23] V.L. Eletsky and J.I. Kapusta, *Phys. Rev.* **C59** (1999) 2757.
- [24] B. Friman and H.J. Pirner, *Nucl. Phys.* **A617** (1997) 496.
- [25] W. Peters, M. Post, H. Lenske, S. Leupold and U. Mosel, *Nucl. Phys.* **A632** (1998) 109.
- [26] R. Rapp, M. Urban, M. Buballa and J. Wambach, *Phys. Lett.* **B417** (1998) 1.
- [27] R. Rapp, *Phys. Rev.* **C63** (2001) 054907.
- [28] H.A. Weldon, *Ann. Phys.* **228** (1993) 43.
- [29] P.F. Kolb and R. Rapp, *Phys. Rev.* **C67** (2003) 044903.
- [30] R. Rapp, *Phys. Rev.* **C66** (2002) 017901.
- [31] E. Kolomeitsev and R. Rapp, in preparation.
- [32] Z. Aouissat, R. Rapp, G. Chanfray, P. Schuck and J. Wambach, *Nucl. Phys.* **A581** (1995) 471.
- [33] D. Lohse, J.W. Durso, K. Holinde and J. Speth, *Nucl. Phys.* **A516** (1990) 513.
- [34] R. Rapp, J.W. Durso and J. Wambach, *Nucl. Phys.* **A596** (1996) 436.
- [35] R. Rapp and J. Wambach, *Phys. Lett.* **B315** (1993) 220.
- [36] F.P. Sassen, S. Krewald and J. Speth, *hep-ph/0212056*.
- [37] G.D. Lafferty, *Zeit. Phys.* **C60** (1993) 659.
- [38] H.W. Barz, G. Bertsch, P. Danielewicz and H. Schulz, *Phys. Lett.* **B275** (1992) 19.
- [39] M. Bleicher, *Proc. of "7. Int. Conference on Strangeness in Quark Matter"* (12.-17.03.03, Atlantic Beach, NC), to be published in *J. Phys.* **G**.
- [40] STAR Collaboration (H. Zhang *et al.*), *Proc. of "7. Int. Conference on Strangeness in Quark Matter"* (12.-17.03.03, Atlantic Beach, NC), to be published in *J. Phys.* **G**.
- [41] STAR Collaboration (C. Adler *et al.*), *Phys. Rev.* **C66** (2002) 061901.
- [42] P. Braun-Munzinger, D. Magestro, K. Redlich and J. Stachel, *Phys. Lett.* **B518** (2001) 41; D. Magestro, *J. Phys.* **G28** (2002) 1745.